Non-intrusive fingerprints extraction from hyperspectral imagery

Longbin Yan[(1,2)], Jie Chen[(2,1)]
[(1)]Centre of Intelligent Acoustics and Immersive Communications
School of Marine Science and Technology, Northwestern Polytechnical University, Xi'an, China
[(2)] Research & Development Institute of Northwestern Polytechnical University, Shenzhen, China
yanlongbin@mail.nwpu.edu.cn dr.jie.chen@ieee.org

***Abstract*—Fingerprint extraction plays an important role in criminal investigation and information security. Conventionally, latent fingerprints are not readily visible and imaging often requires to use intrusive manners. Hyperspectral imaging techniques provide a possibility to extract fingerprints in a non-intrusive manner, however it requires well-designed image analysis algorithms. In this paper, we consider the problem of fingerprint extraction from hyperspectral images and propose a processing scheme. The proposed scheme extracts image textures by local total variation (LTV) and uses Histogram of Oriented Gradient (HOG) information to fuse these channels. Experiment results with a real image show the ability of the proposed method for extracting fingerprints from complex backgrounds.**

***Index Terms*—Fingerprint extraction, hyperspectral images, local total variation, texture, histogram of oriented gradient**

I. Introduction

A fingerprint is a very recognized and acceptable security feature. It is conventionally used for human identification and criminal vetting. Fingerprints can be found on practically any solid surface, and they can be classified two categories according to their visibility. Visible fingerprints are formed when blood or ink is transferred from a finger or thumb to a surface. Latent fingerprints can be found on a wide variety of surfaces, and they are formed when the bodys natural oils and sweat on the skin are deposited onto another surface.

It is worth noting that latent fingerprints are not readily visible and imaging often requires the use of fingerprint powders, chemical reagents, in an intrusive manner. With the advance of the imaging device, it is now possible to perform a non-intrusive print extraction process via the hyperspectral imaging technology. Hyperspectral imaging provides 2-D spatial images over many contiguous bands. Rich spectral information endows hyperpectral imaging with the ability to perform detection, classification and analysis that can not be achieved over conventional color images. This area has received considerable attention in the last decade. Applications include remote sensing [1], food security [2], anomaly detection [3], crop detection [4], identification of cultural relics [5], medical diagnosis [6], [7], atmospheric monitoring [8], etc [9]–[11]. In [12], [13], they focused on fingerprints extraction of latent fingerprints that can be distinguished conveniently from spectral information. Hyperspectral imaging can thus serve as a powerful tool for non-intrusive extraction for either visible or latent fingerprints.

This work was supported in part by Natural Science Foundation of Shenzhen under grant JCYJ2017030155315873, and the Seed Foundation of Innovation and Creation for Graduate Students in Northwestern Polytechnical University.

Most conventional fingerprint extraction/segmentation algorithms are applied to gray images. Typically, these techniques are based on the local texture direction of the image [14]. In [15], an algorithm is proposed to extract features of fingerprints by using Gabor filter bank. In [16], the authors presented a combined feature level and score level fusion Gabor filter-based approach. In [17], a dictionary-based approach is proposed for automatic latent segmentation and enhancement. In [18], the authors proposed to construct the dictionary by region wise to correct the orientation field in latent image. Unfortunately, none of them combine spectral information with texture information. In [19], Zhang et al. proposed a adaptive directional total variation (ADTV) image decomposition scheme for latent fingerprint segmentation.

All of the above mentioned methods neither process multi-channel data, not use spectral signatures of materials, they can not be directly applied to the fingerprint extraction from hyperspectral images. In this paper, we firstly describe the problem of extracting fingerprints from hyperspectral data, and propose an algorithm to perform this task. The proposed algorithm first generate the texture images of each channel by calculating LTV, and then use HOG to compute weights associated to data cells for each channel. The extracted fingerprint will be obtained by fusing all channels with these weights. The proposed scheme benefits from the desired fingerprint texture of each channel and provides promising extraction results.

II. Data structure and problem description

A hyperspectral image is a three dimensional data cube. Suppose that the raw image under study is denoted by $\boldsymbol{X}''$, which has w pixels in each row and h pixels in each column. Each pixel consists of a reflectance vector in L contiguous spectral bands. Further we use superscript $^{(k)}$ to denote the kth channel of the data.

A fingerprint generally presents an a concentric-whorl alike pattern with a a series of small grooves and valleys.

ISBN 978-90-827970-1-5 © EURASIP 2018

However complex background may damage distinct parts of this pattern on each reflectance channel. Our objective is to extract fingerprints by appropriately fusing the textures and removing unrelated objects using multiple channel information in the scene under study. Compared to conventional images, three dimensional hyperspectral data can be beneficial in the following two senses for extracting a fingerprint:

1) It is possible to use spectral signatures to detect a fingerprint, or to rule out unrelated backgrounds. While the former operation is mainly applied to visible fingerprints, and the latter can be applied to both visible and latent cases.
2) Though a fingerprint pattern may not be complete in a single channel, it is possible to benefit multi-channel information to fuse textures and form a complete fingerprint target.

III. Fingerprint extraction from a hyperspectral image

In this section, we propose a scheme for extracting fingerprints from a hyperspectral image.

A. Data preprocessing and dimension reduction

Data preprocessing mainly includes noise reduction and normalization process. For an image with significant acquisition noise it can be beneficial to apply a Gaussian filter or a median filter to remove noise. A further grey level transformation can also be applied to the image to enhance the contrast, specially for regions where fingerprints present, to facilitate the further processing. For example, the logarithm transformation will be used in our illustrative example in Sec. IV. We denote the this step by

$$\boldsymbol{X}'' \in \mathbb{R}^{h\times w\times L} \xrightarrow{\text{Preprocessing}} \boldsymbol{X}' \in \mathbb{R}^{h\times w\times L}. \tag{1}$$

Hyperspectral data provides us with rich spectral information that is favorable for target detection, extraction tasks. However it can be computational cumbersome to perform analysis over all channels because of spectral redundancy in data. This implies the necessity of reducing the data size over the spectral dimension. The most popular technique to perform this task is principal-component analysis (PCA). PCA allows us to generate principal components with dimension $\ell < L$ without any priori information. If priori knowledges of background materials are known, it is also possible to use spectral unmixing techniques to perform the background removal.

We denote this step by

$$\boldsymbol{X}' \in \mathbb{R}^{h\times w\times L} \xrightarrow{\text{Dim. reduction}} \boldsymbol{X} \in \mathbb{R}^{h\times w\times \ell}. \tag{2}$$

B. Channel-wise texture extraction

We then perform the texture extraction on each channel $\boldsymbol{X}^{(k)}$, since fingerprints present as a particular texture in image. Consider that an image can be decomposed as

$$\boldsymbol{X}^{(k)} = \boldsymbol{U}^{(k)} + \boldsymbol{V}^{(k)}, \tag{3}$$

where we write $\boldsymbol{X}^{(k)}$ as the sum of is cartoon component $\boldsymbol{U}^{(k)}$ and texture component $\boldsymbol{V}^{(k)}$. We use the LTV-based technique proposed in [20] to compute this decomposition. LTV of $\boldsymbol{X}^{(k)}$ is defined by

$$\mathrm{LTV}_\sigma(\boldsymbol{X}^{(k)}) = L_\sigma \circ \left|\nabla \boldsymbol{X}^{(k)}\right| \tag{4}$$

with L_σ being a low-pass filter with cut-off radius σ, and ∇ being the gradient operator. Thus, a function that indicates texture trend in the neighborhood of (i,j)th pixel of $\boldsymbol{X}^{(k)}$ can be defined as

$$\lambda_{\sigma,ij} = \frac{\left[\mathrm{LTV}_\sigma(\boldsymbol{X}^{(k)}) + \mathrm{LTV}_\sigma(L_\sigma \circ \boldsymbol{X}^{(k)})\right]_{ij}}{\left[\mathrm{LTV}_\sigma(\boldsymbol{X}^{(k)})\right]_{ij}} \tag{5}$$

$\lambda_{\sigma,ij}$ is called the local total variation reduction rate, ranging from 0 to 1. A rate tending 0 to suggests that the (ij)th pixel belongs to the cartoon image. A rate tending 1 suggests that the (i,j)th pixel belongs to the texture image. Thus, the texture and the cartoon image can be distinguished by a weight function based on the LTV reduction rate, namely

$$[\boldsymbol{U}^{(k)}]_{ij} = \omega(\lambda_{\sigma,ij})\left[L_\sigma \circ \boldsymbol{X}^{(k)} - \boldsymbol{X}^{(k)}\right]_{ij} + [\boldsymbol{X}^{(k)}]_{ij} \tag{6}$$

where $\omega(\cdot)$ is the soft threshold function given by

$$\omega(y) = \begin{cases} 0, y \le a_1 \\ (y-a_1)/(a_2-a_1), a_1 \le y \le a_2 \\ 1, y \ge a_2 \end{cases} \tag{7}$$

and parameters a_1, a_2 are usually fixed to 0.25 and 0.5. Finally, the texture component associated to kth channel is obtained by

$$\boldsymbol{V}^{(k)} = \boldsymbol{X}^{(k)} - \boldsymbol{U}^{(k)}, \text{ for } k \in \{1,\dots,\ell\}. \tag{8}$$

C. Multichannel texture fusion

Note that texture components $\boldsymbol{V}^{(k)}$ contain fingerprints along with other high frequency components of the image. It is then necessary to fuse all $\{\boldsymbol{V}^{(k)}\}_{k=1}^{\ell}$ from all channels to complete fingerprints as well as to remove unrelated textures. To achieve this objective, we propose an HOG-based multichannel texture fusion method in this subsection.

We present each texture component $\boldsymbol{V}^{(k)}$ by a partition consisting of non-overlapping cells $\boldsymbol{V}_{ij}^{(k)}$ of size $m \times m$, namely

$$\boldsymbol{V}^{(k)} = \begin{bmatrix} \boldsymbol{V}_{11}^{(k)} & \cdots & \boldsymbol{V}_{1\frac{w}{m}}^{(k)} \\ \vdots & \ddots & \vdots \\ \boldsymbol{V}_{\frac{h}{m}1}^{(k)} & \cdots & \boldsymbol{V}_{\frac{h}{m}\frac{w}{m}}^{(k)} \end{bmatrix} \tag{9}$$

where we assume that $\frac{h}{m}$ and $\frac{w}{m}$ are integers without loss of generality. Computing the gradient of each cell in x-direction and y-direction leads to gradient $\nabla_x \boldsymbol{V}_{ij}^{(k)}$ and $\nabla_y \boldsymbol{V}_{ij}^{(k)}$. For any pixel s of $\boldsymbol{V}_{ij}^{(k)}$, the amplitude of the gradient at this pixel is given by

$$\psi_{ij}^{(k)}(s) = \sqrt{[\nabla_x \boldsymbol{V}_{ij}^{(s)}(s)]^2 + [\nabla_y \boldsymbol{V}_{ij}^{(k)}(s)]^2}, \tag{10}$$

ISBN 978-90-827970-1-5 © EURASIP 2018

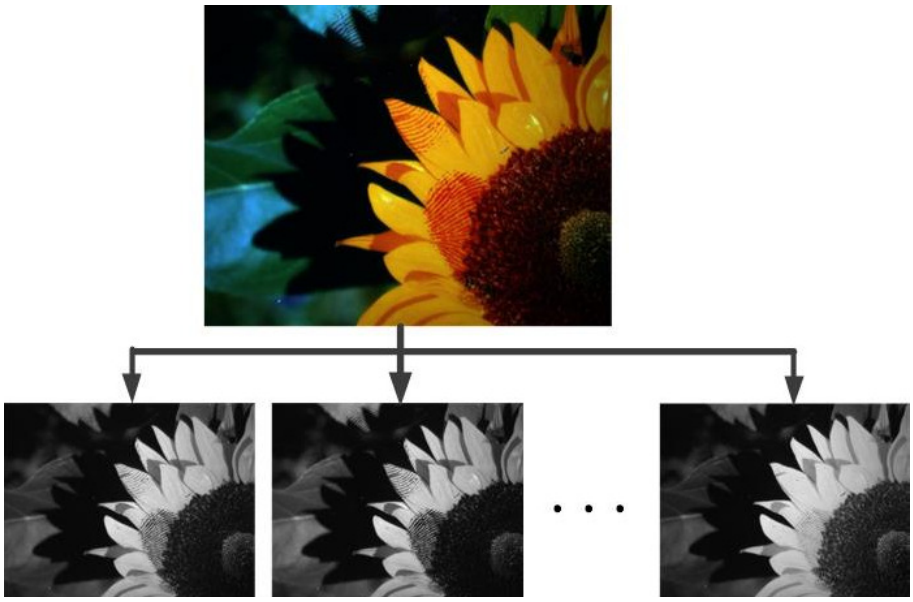

Fig. 1. Illustrative example with a real hyperspectral image. Upper: false color image. Bottom: examples of channels. Capturing parameters are shown in Table. 1

and the angle is given by

$$\theta_{ij}^{(k)}(s) = \tan^{-1} \nabla_y \boldsymbol{V}_{ij}^{(k)}(s) / \nabla_x \boldsymbol{V}_{ij}^{(k)}(s). \tag{11}$$

We then generate the vector $\boldsymbol{h}_{ij}^{(k)} \in \mathbb{R}^{\kappa}$ of HOG, whose entries are given by

$$\begin{aligned} [\boldsymbol{h}_{ij}^{(k)}]_p = & \sum_{\{s:\theta_{ij}^{(k)}(s) \in \mathcal{I}_p\}} |\psi_{ij}^{(k)}(s)| \\ & \text{with } \mathcal{I}_p = [\pi(p-1)/\kappa, p\pi/\kappa] \\ & (p = 1, 2, ..., \kappa) \end{aligned} \tag{12}$$

The gradient direction is more consistent in cells where local parts of a fingerprint appear, leading to a concentrated support set of $\boldsymbol{h}_{ij}^{(k)}$. A cell with random gradient directions results in more uniformly distributed entries of $\boldsymbol{h}_{ij}^{(k)}$. This implies the entries of $\boldsymbol{h}_{ij}^{(k)}$ corresponding to a cell with partial fingerprints tends to have a larger variance. Therefore, it is reasonable to use such a variance to rule out non-print cells, and derive combination weights to fuse all channels. Let the variance of $\boldsymbol{h}_{ij}^{(k)}$ be denoted by $\sigma^2(\boldsymbol{h}_{ij}^{(k)})$, we propose to calculate the combination weights with the following rule:

$$\omega_{ij}^{(k)} = \begin{cases} \dfrac{\sigma^2(\boldsymbol{h}_{ij}^{(k)})}{\sum_{q=1}^{\ell} \sigma^2(\boldsymbol{h}_{ij}^{(q)})} & \text{if } \sigma^2(\boldsymbol{h}_{ij}^{(k)}) \geq \bar{\sigma} \\ 0 & \text{otherwise.} \end{cases} \tag{13}$$

where $\bar{\sigma}$ is a user-defined threshold to determine whether the current cell contains fingerprint features. Considering the weight matrix $\boldsymbol{\Omega}^{(k)}$ with (ij)th entry given by $\omega_{ij}^{(k)}$, we perform the erosion and dilation operations to $\boldsymbol{\Omega}^{(k)}$ for removing noisy interferences and filling holes in the target area. The weights after operation are denoted by adding a tilde such that $\widetilde{\omega}_{ij}^{(k)}$. Finally the output image that segments fingerprints is obtained by fusing ℓ channels with these weights:

$$\boldsymbol{O} = \begin{bmatrix} \sum_{k=1}^{\ell} \widetilde{\omega}_{11}^{(k)} \boldsymbol{V}_{11}^{(k)} & \cdots & \sum_{k=1}^{\ell} \widetilde{\omega}_{1\frac{w}{m}}^{(k)} \boldsymbol{V}_{1\frac{w}{m}}^{(k)} \\ \vdots & \ddots & \vdots \\ \sum_{k=1}^{\ell} \widetilde{\omega}_{\frac{h}{m}1}^{(k)} \boldsymbol{V}_{\frac{h}{m}1}^{(k)} & \cdots & \sum_{k=1}^{\ell} \widetilde{\omega}_{\frac{h}{m}\frac{w}{m}}^{(k)} \boldsymbol{V}_{\frac{h}{m}\frac{w}{m}}^{(k)} \end{bmatrix} \tag{14}$$

TABLE I
THE PARAMETERS OF HYPERSPECTRAL IMAGING

Parameters	Value
Wavelength range (nm)	$420 - 720$
Spectral resolution (nm)	$8 - 20$
Image spatial size (pixels)	512×640
Number of channels	31
Field	$0 - \pm 7^{\circ}$

IV. Experiment results

In this section, we validate the proposed hyperspectral fingerprint extraction scheme via a real image. This image was captured in our laboratory with a GaiaField hyperspectral device. The scenario contained several pieces of leaves and a flower. Two fingerprints presented in this scenario. The first one was located on the upper-middle part with leaves and petals as background, the other was located on the lower-right part with petals and stamens as background. The false color image is shown on the upper part of Fig. 1. Note that due to the space limitation, though we only illustrate the proposed scheme with this single image, this scene has a sufficiently complex interaction between the target and background and can be typical difficult problem for fingerprint extraction. It is clear that the fingerprints in this scenario can not be easily

ISBN 978-90-827970-1-5 © EURASIP 2018

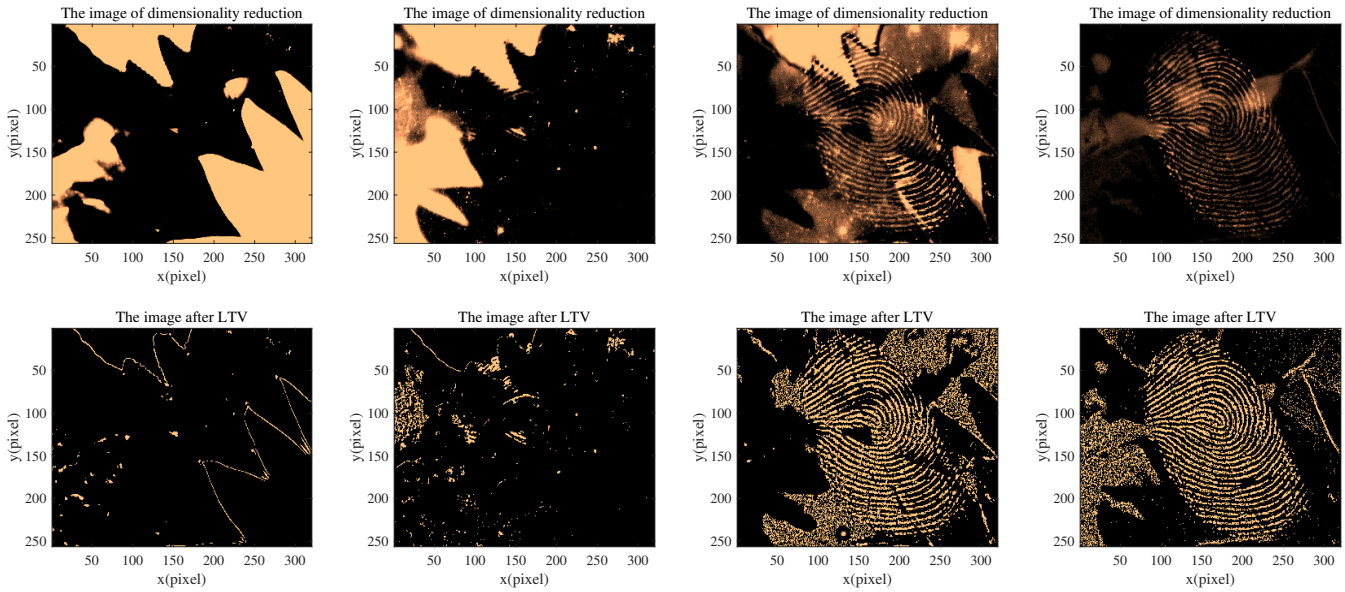

Fig. 2. Intermediate results of processing, using the upper part of the image. From left to right: 4 data channels after PCA. From top to bottom: channel images after PCA, images after LTV.

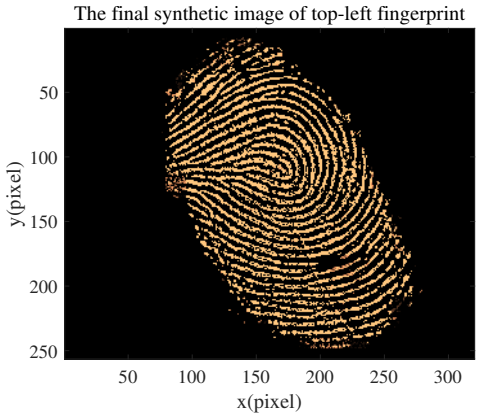

(a) Fingprint-1

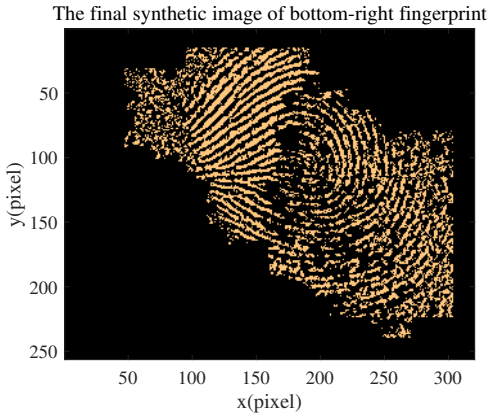

(b) Fingprint-2

Fig. 3. Final extraction results.

extracted with conventional techniques. The parameters of this hyperspectral data is reported in Table 1. Specifically we notice that the image has $L = 31$ spectral channels. Three exemplary channel images are shown in the lower part of Fig. 1.

We then performed the proposed scheme. In the preprocessing step, we used the logarithm transformation

$$f(x) = \log(1 + x) \tag{15}$$

to adjust the contrast of each channel. Dimension reduction was performed via PCA. Considering eigenvalues that take 99% of total energy leads to $\ell = 4$. The cell size was set to $m = 8$, and the dimension of HOG vector was set to $\kappa = 9$. Threshold $\bar{\sigma}$ was set to 0.4. The intermediate processing results are illustrated in Fig. 2 with a sub-region of the image. Finally extraction results of these two fingerprints are shown in Fig 3. This example shows the capacity of the proposed method for extracting fingerprints from complex backgrounds.

V. Conclusion

Non-intrusive fingerprint extraction can be an important application in practice. In this paper we proposed a method to extract fingerprints from hyperspectral images. We used LTV to compute the texture images of each channel, then used HOG to compute weights to fuse the channels. Experiments with a real hyperspectral image with complex backgrounds validated the proposed algorithm. Future work will include using supervised techniques to enhance the extraction performance, creating a hyperspectral image database for fingerprints, and validating algorithms with this database.

ISBN 978-90-827970-1-5 © EURASIP 2018

REFERENCES

[1] Y. Liu, N. Wang, L. Ma, C. Li, and L. Tang, "A method for atmospheric parameters and surface reflectance retrieval from hyperspectral remote sensing data," in *Proc. IEEE. WHISPERS*, Jun. 2015, pp. 1–4.

[2] X. Ye, K. Iino, S. Zhang, and S. Oshita, "Nondestructive monitoring of chicken meat freshness using hyperspectral imaging technology," in *Proc. IEEE. WHISPERS*, Jun. 2015, pp. 1–4.

[3] M. D, R. Guerra, S. Lpez, and R. Sarmiento, "An algorithm for an accurate detection of anomalies in hyperspectral images with a low computational complexity," *IEEE Trans. Geosci. Remote Sens.*, vol. PP, no. 99, pp. 1–18, 2017.

[4] J. Jiang, Y. Chen, J. Zhang, and J. Li, "Using hyperspectral indices to diagnose severity of winter wheat stripe rust," in *Proc. IEEE. ICOSP*, Oct. 2006, vol. 1.

[5] Y. Tan and M. Hou, "Analyzing stains on calligraphy and painting using hyperspectral imaging," in *Proc. IEEE. EORSA*, Jul. 2016, pp. 157–160.

[6] H. Akbari, Y. Kosugi, K. Kojima, and N. Tanaka, "Detection and analysis of the intestinal ischemia using visible and invisible hyperspectral imaging," *IEEE Trans. Biomedical Engineering*, vol. 57, no. 8, pp. 2011–2017, Aug 2010.

[7] H. Akbari, Y. Kosugi, K. Kojima, and N. Tanaka, "Hyperspectral imaging and diagnosis of intestinal ischemia," in *Proc. IEEE. IEMBS*, Aug 2008, pp. 1238–1241.

[8] R. Shobiga and J. Selvakumar, "Survey on properties and accuracy assessment of climate changes using hyperspectral imaging," in *Proc. IEEE. ICGET*, Nov 2015, pp. 1–6.

[9] Y. Q. Zhao, L. Zhang, and S. G. Kong, "Band-subset-based clustering and fusion for hyperspectral imagery classification," *IEEE Trans Geosci. Remote Sens.*, vol. 49, no. 2, pp. 747–756, Feb 2011.

[10] V. Saini and A. K. Patel, "Identification of craters on lunar surface using hyperspectral chandrayan data," in *Proc. IEEE. WHISPERS*, Jun. 2015, pp. 1–4.

[11] A. Ertrk, M. D. Iordache, and A. Plaza, "Hyperspectral change detection by sparse unmixing with dictionary pruning," in *Proc. IEEE. WHISPERS*, Jun. 2015, pp. 1–4.

[12] S. Cadd, B. Li, P. Beveridge, W. T. OHare, A. Campbell, and M. Islam, "The non-contact detection and identification of blood stained fingerprints using visible wavelength hyperspectral imaging: Part ii effectiveness on a range of substrates," *Science and Justice*, vol. 56, no. 3, pp. 191–200, Jan 2016.

[13] A. Nakamura, H. Okuda, T. Nagaoka, N. Akiba, K. Kurosawa, K. Kuroki, F. Ichikawa, A. Torao, and T. Sota, "Portable hyperspectral imager with continuous wave green laser for identification and detection of untreated latent fingerprints on walls," *Forensic science international*, vol. 254, pp. 100–105, Sep 2015.

[14] T. Ohtsuka, D. Watanabe, D. Tomizawa, Y. Hasegawa, and H. Aoki, "Reliable detection of core and delta in fingerprints by using singular candidate method," in *Proc.IEEE CVPRW*, Jun. 2008, pp. 1–6.

[15] S. Chavan, P. Mundada, and D. Pal, "Fingerprint authentication using gabor filter based matching algorithm," in *Proc. IEEE. ICTSD*, Feb 2015, pp. 1–6.

[16] F. Kaggwa, J. Ngubiri, and F. Tushabe, "Combined feature level and score level fusion gabor filter-based multiple enrollment fingerprint recognition," in *Proc. IEEE. SCOPES*, Oct 2016, pp. 159–165.

[17] K. Cao, E. Liu, and A. K. Jain, "Segmentation and enhancement of latent fingerprints: A coarse to fine ridgestructure dictionary," *IEEE Trans. Pattern Analysis Machine Intelligence*, vol. 36, no. 9, pp. 1847–1859, Sep 2014.

[18] S. Kumar and R. L. Velusamy, "Latent fingerprint preprocessing: Orientation field correction using region wise dictionary," in *Proc. IEEE. ICACCI*, Aug 2015, pp. 1238–1243.

[19] J. Zhang, R. Lai, and C. J. Kuo, "Adaptive directional total-variation model for latent fingerprint segmentation," *IEEE Trans. Information Forensics and Security*, vol. 8, no. 8, pp. 1261–1273, Aug 2013.

[20] A. Buades, T. M. Le, J. M. Morel, and L. A. Vese, "Fast cartoon + texture image filters," *IEEE Trans. Image Process.*, vol. 19, no. 8, pp. 1978–1986, Aug 2010.

ISBN 978-90-827970-1-5 © EURASIP 2018